HHS Public Access

Author manuscript

Cancer Res. Author manuscript; available in PMC 2018 February 01.

Published in final edited form as:

Cancer Res. 2017 February 01; 77(3): 742–752. doi:10.1158/0008-5472.CAN-16-1817.

Pifithrin-μ prevents cisplatin-induced chemobrain by preserving neuronal mitochondrial function

Gabriel S. Chiu, **Magdalena A. Maj**, **Sahar Rizvi**, **Robert Dantzer**, **Elisabeth G. Vichaya**, **Geoffroy Laumet**, **Annemieke Kavelaars**, and **Cobi J. Heijnen**

Laboratory of Neuroimmunology, Department of Symptom Research, The University of Texas MD Anderson Cancer Center, Houston, Texas

Abstract

Cognitive impairment termed chemobrain is a common neurotoxicity associated with chemotherapy treatment, affecting an estimated 78% of patients. Prompted by the hypothesis that neuronal mitochondrial dysfunction underlies chemotherapy-induced cognitive impairment (CICI), we explored the efficacy of administering the small molecule pifithrin (PFT)-μ, an inhibitor of mitochondrial p53 accumulation, in preventing CICI. Male C57BL/6J mice injected with cisplatin +/− PFT-μ for two 5-day cycles were assessed for cognitive function using novel object/place recognition and alternation in a Y-maze. Cisplatin impaired performance in the novel object/place recognition and Y-maze tests. PFT-μ treatment prevented CICI and associated cisplatin-induced changes in coherency of myelin basic protein fibers in the cingular cortex and loss of doublecortin^{+} cells in the subventricular zone and hippocampal dentate gyrus. Mechanistically, cisplatin decreased spare respirator capacity of brain synaptosomes and caused abnormal mitochondrial morphology, which was counteracted by PFT-μ administration. Notably, increased mitochondrial p53 did not lead to cerebral caspase-3 activation or cytochrome-c release. Furthermore, PFT-μ administration did not impair the anticancer efficacy of cisplatin and radiotherapy in tumor-bearing mice. Our results supported the hypothesis that neuronal mitochondrial dysfunction induced by mitochondrial p53 accumulation is an underlying cause of CICI, and that PFT-μ may offer a tractable therapeutic strategy to limit this common side-effect of many types of chemotherapy.

Keywords

Chemobrain; cognition; cisplatin; mitochondria; brain damage

INTRODUCTION

Advances in the efficacy of cancer treatment have led to a sharp increase in the number of cancer survivors, which has reached nearly 15 million in the United States alone[1], [2]. However, in many cases cancer treatment is associated with severe neurotoxic side effects,

Correspondence: Cobi J. Heijnen, PhD, Laboratory of Neuroimmunology, Department of Symptom Research, The University of Texas MD Anderson Cancer Center, 1515 Holcombe Boulevard, Unit 384, Houston, TX 77030.

Conflicts of Interest: The authors report no conflicts of interest in this work.

including fatigue, peripheral pain [3], paresthesia, and cognitive deficits, that can persist long after completion of treatment [4]. These neurotoxicities not only disrupt social, educational, and occupational functioning, but also decrease survival by interfering with adherence to medication and health behavior.

In humans, chemotherapy-induced cognitive impairment (CICI), so-called “chemobrain,” is characterized by subtle to moderate cognitive deficits, including a decrease in processing speed, memory, executive functioning, and attention, as assessed by neuropsychological tests [4]–[6]. CICI has been noted in 78% of cross-sectional and 69% of prospective longitudinal studies performed between 1995 and 2012 in patients treated for breast cancer [7]–[9]. One in two adults is projected to be diagnosed with cancer in his or her lifetime, implying that CICI represents a growing public health concern.

Advanced neuroimaging techniques have revealed that chemotherapy causes structural alterations in white and gray matter in patients with cancer, along with an increased level of activation of the fronto-parietal attentional network [5]. However, little is known about the mechanism underlying CICI, and no preventive or curative interventions have been approved by the US Food and Drug Administration.

Platinum-based chemotherapeutic agents like cisplatin are widely used to treat solid tumors [10]. Traditionally, these agents are thought to act on tumor cells by preferential binding to the guanine residues in DNA to induce crosslinking [11]. The body’s subsequent inability to repair damaged DNA leads to an arrest in mitosis, inhibition of cell proliferation, and tumor cell death.

Preclinical studies have shown that cisplatin crosses the blood–brain barrier and impairs adult neurogenesis in the brain [12]. We recently showed that cisplatin-induced cognitive impairment in mice was associated with increased coherency of white-matter structures and sharp decrease in the number of neuronal dendritic spines and arborizations [2].

In rodent models, peripheral neuropathy induced by cisplatin or other chemotherapeutic agents such as taxanes is associated with structural damage to mitochondria in the dorsal root ganglia and peripheral nerves [13]. In general, damaged mitochondria can give rise to increased oxidative stress, inflammation, and pro-apoptotic signaling [14]. We recently showed that co-administration of the small molecule pifithrin (PFT)-μ, an inhibitor of mitochondrial p53 accumulation, protects against taxane-induced and cisplatin-induced peripheral neuropathy[3]. In addition, we have demonstrated that PFT-μ is neuroprotective in a model of neonatal hypoxic–ischemic brain damage by preventing neuronal apoptosis [15].

In this study, we investigated whether cerebral neuronal mitochondrial damage is the underlying mechanism of cisplatin-induced cognitive impairment. Moreover, we tested whether PFT-μ is capable of preventing the development of cisplatin-induced chemobrain and precluding structural alterations in the brain with respect to damage to white matter and neurogenic areas in the brain.

MATERIALS AND METHODS

Animals

C57BL/6J male mice were used in this study. Mice were bred in-house and were allowed water and food *ad libitum*. Housing was kept constant at 22 ± 2°C, and a 12/12 h reverse dark–light cycle (dark 1000–2200 h) was employed. Video recording of animal behavior was performed under red light using a Sony Handycam DCR-SR100.

All experiments were conducted at The University of Texas MD Anderson Cancer Center in Houston, Texas. Animal usage was carried out in accordance with Institutional Animal Care and Use Committee-approved protocols.

Injections

Cisplatin (2.3 mg/kg; Fresenius Kabi USA, Lake Zurich, IL) or phosphate-buffered saline (PBS) was administered intraperitoneally (i.p.) daily for 5 days, followed by a 5-day rest with no injection and then another 5-day injection cycle. To investigate the effects of PFT-μ on cognitive function, PFT-μ (8 mg/kg; Sigma-Aldrich/Millipore Sigma, St. Louis, MO) or vehicle (5% dimethyl sulfoxide in saline) was administered i.p. 1 h prior to cisplatin injection.

Novel Object/Place Recognition and Y-Maze Tests

To assess cognitive function, we subjected mice to novel object/place recognition (NOPR) and Y-maze tests 7 days after the final cisplatin injection. All behavioral assays were performed in a blinded setup. NOPR was performed as we have previously described [2]. In brief, mice were transferred to a testing arena (46.99 cm × 25.4 cm) containing two identical objects placed against one side of the arena for 5 min (training phase) and then returned to their home cages for 30 min. Mice were transferred back to the arena, now containing one familiar object placed at the same location as in training, and one novel object placed on the opposite end of the arena (testing phase). Investigative behavior toward either object during the 5 min testing period was evaluated using EthoVision XT 10.1 video tracking software (Noldus Information Technology Inc., Leesburg, VA). Discrimination index was determined by the equation $(T_{Novel} - T_{Familiar})/(T_{Novel} + T_{Familiar})$.

For the Y-maze test, spontaneous alternations were performed as previously described [16]. In brief, mice were placed in a symmetrical three-arm, gray plastic Y-maze (35 cm length × 5 cm width × 15.5 cm height per arm, with an arm angle of 120°) with external spatial room cues. Mice were randomly placed in one of the arms. Movement was recorded for 5 min, and mouse exploration was evaluated. Perfect alternations were defined as exploration of all three arms sequentially before reentering a previously visited arm. All four paws must have been within the arm to be counted as an entrance. Results are represented as the ratio of the number of perfect alternations to the total number of possible alternations.

Locomotion

Spontaneous locomotor activity was measured as described previously [16]–[20]. In brief, mice were video recorded for 5 min in their home cage. Distance travelled was quantified using EthoVision XT 10.1 (Noldus Information Technology, Inc.).

Body Weight

Body weights were measured daily at the time of injection. Percent change from baseline (day 0) was calculated.

Tumor Response to Chemoradiation

We used a heterotopic syngeneic murine model of human papilloma virus (HPV)-related head and neck cancer to assess whether PFT-μ might potentially interfere with the tumor's response to chemoradiation [21]–[23]. Male C57BL/6J mice were injected in the hind leg with 1×10^6 cells derived from C57BL/6 oropharyngeal epithelial cells that were transfected with oncogenes E6/7 of HPV 16 and hRAS [21], [22]. Mice were injected with PFT-μ (8 mg/kg) or vehicle 24 h prior to a curative regimen of cisplatin (5.28 mg/kg i.p.; Calbiochem, EMD Millipore, Billerica, MA) and local irradiation (8 Gy provided by a small animal cesium^{137} irradiator that collimates parallel opposed radiation beams to a 3 cm field) starting 12 days after tumor implantation and repeated weekly for 3 weeks [22]. Tumor volume was determined using Vernier calipers from three mutually orthogonal tumor diameters, where volume = $(\pi/6)(d1*d2*d3)$.

Quantitative Real-Time Polymerase Chain Reaction

Chemotherapy is thought to induce a low-grade inflammation in patients with cancer that may contribute to neurotoxic side effects, including cognitive dysfunction [24]–[26]. We analyzed the effect of cisplatin on the expression of certain prototypic pro-inflammatory cytokines and glial activation markers in the hippocampus and frontal cortex at the mRNA level. RNA was isolated as described previously [16], [18], [20]. In brief, mice were perfused postmortem with ice-cold PBS, and the hippocampus and prefrontal cortex were dissected from whole brain. RNA was reverse transcribed using the High-Capacity cDNA Reverse Transcription Kit (Applied Biosystems/Thermo Fisher Scientific, Waltham, MA). The Prime Time qPCR Assays used were interleukin (IL)-1β (NM_008361(1)), IL-6 (NM_031168(1)), tumor necrosis factor (TNF)-α (NM_013693(1)), CD11b (*Itgam*) (NM_008401(2)), glial fibrillary acidic protein (GFAP) (NM_010277(1)), and glyceraldehyde 3-phosphate dehydrogenase (GAPDH) (NM_008084(1)) (Integrated DNA Technologies, Coralville, IA). Quantitative real-time polymerase chain reaction (qRT-PCR) was performed on a CFX384 Real-Time System (Bio-Rad Laboratories, Hercules, CA) using TaqMan Universal PCR Master Mix (Applied Biosystems).

Immunohistochemistry

The integrity of the neurogenic stem cell niche is crucial for adequate cognitive function [27], [28]; we have found that cisplatin reduces white-matter integrity as analyzed at the level of the coherency of myelin basic protein (MBP) fibers in the cingulate cortex [2]. We therefore performed fixation and immunostaining of neuronal precursors in the

subventricular zone (SVZ) and dentate gyrus (DG), as previously described [3]. In brief, mice were perfused with 4% paraformaldehyde (PFA). Brains were removed and fixed in 4% PFA for 48 h, then paraffin embedded and sectioned at 8 μm for the SVZ and cingulum and 10 μm for the DG. Sectioned were stained for doublecortin (DCX, 1:50; Abcam, Cambridge, UK) and MBP (1:100; Abcam). Images were taken at 40× and 63× objectives and quantified for positive staining using ImageJ. Cell counting was performed by two experienced and independent researchers blinded to treatment.

Synaptosome Isolation

To study whether cisplatin treatment resulted in altered mitochondrial morphology at the time of the behavioral analyses, we prepared synaptosomes of the brains of mice at 7–9 days after the last dose of cisplatin. Synaptosomes were isolated according to Kamat et al. [29]. Briefly, after perfusion with PBS, brains were dissected and homogenized (10% w/v) into a 0.32 M sucrose 4-(2-hydroxyethyl)-1-piperazineethanesulfonic acid (HEPES) buffer (145 mM NaCl, 5 mM KCl, 2 mM $CaCl_2$, 1 mM $MgCl_2$, 5 mM glucose, 5 mM HEPES, pH 7.4) using a glass Dounce homogenizer with ~10 up-and-down strokes. The brain lysate was centrifuged at 4°C for 10 min at 1000× *g*. The supernatant was extracted and diluted 1:1 with 1.3 M sucrose HEPES buffer (final concentration of 0.8 M sucrose) and centrifuged at 4°C for 30 min at 20,000× *g*. The pellet containing isolated synaptosomes was resuspended in base media (Seahorse Biosciences/Agilent Technologies, Santa Clara, CA) supplemented with 11 mM glucose, 2 mM glutamine, and 1 mM pyruvate for oxygen-consumption analysis or 2% glutaraldehyde plus 2% PFA in PBS for transmission electron microscopy.

Transmission Electron Microscopy

Similar to methods we have previously described [3], synaptosomes were isolated and fixed in a solution containing 2% glutaraldehyde plus 2% PFA in PBS for at least 24 h. Samples were then fixed with a solution containing 3% glutaraldehyde plus 2% PFA in 0.1 M cacodylate buffer, pH 7.3, then washed in 0.1 M sodium cacodylate buffer and treated with 0.1% Millipore-filtered cacodylate-buffered tannic acid, post-fixed with 1% buffered osmium tetroxide for 30 min, and stained en bloc with 1% Millipore-filtered uranyl acetate. The samples were dehydrated in increasing concentrations of ethanol, infiltrated, and embedded in LX-112 medium. The samples were polymerized in a 60°C oven for approximately 2 days. Ultrathin sections were cut in a Leica Ultracut microtome (Leica Microsystems Inc., Deerfield, IL), stained with uranyl acetate and lead citrate in a Leica EM Stainer, and examined in a JEM 1010 transmission electron microscope (JEOL, USA, Inc., Peabody, MA) at an accelerating voltage of 80 kV. Digital images were obtained using AMT Imaging System (Advanced Microscopy Techniques Corp, Danvers, MA). Quantifications were performed by two independent researchers using ImageJ.

Oxygen Consumption Rate

To determine whether the mitochondrial morphological abnormalities induced by cisplatin treatment and the protective effects of PFT-μ were associated with changes in mitochondrial bioenergetics, we analyzed synaptosomal oxygen consumption rates (OCR) using the Seahorse XFe 24 analyzer. Synaptosomes were isolated and plated at 50 μg of total protein on a Seahorse XFe 24 microplate (Seahorse Biosciences) pre-coated with GelTrex (1 hour in

37°C; Life Technologies/Thermo Fisher Scientific). The plate was centrifuged at 600× *g* for 30 min and then allowed to rest at 37°C for 30 min. The assay cartridge was loaded with 4 μM oligomycin in Port A, 6 μM carbonyl cyanide 4-(trifluoromethoxy)phenylhydrazone (FCCP) in Port B, and 2 μM of rotenone and 2 μM of antimycin A in Port C. The decrease in OCR in response to addition of the complex-III inhibitor oligomycin represents oxygen consumption related to ATP production, whereas the uncoupler FCCP induces maximal OCR. The addition of rotenone/antimycin A inhibits all mitochondrial respiration, leaving only non-mitochondrial oxygen consumption. All values were normalized to mitochondrial-dependent respiration.

Mitochondrial Isolation

To investigate the mechanism underlying the protective effect of PFT-μ, we examined the effect of cisplatin on mitochondrial p53 and on heat-shock protein 70 (HSP70), a secondary target of PFT-μ in proliferating tumor cells [30], [31]. Because it is generally accepted that increases in mitochondrial p53 induce apoptosis through mitochondrial outer membrane permeabilization, leading to activation of caspase-3 and subsequent apoptosis [32], we also examined the effect of cisplatin treatment on brain cytosolic cytochrome-c and activation of caspase-3.

Brains were pulverized using liquid nitrogen-cooled mortar and pestle. Approximately 100 mg of brain sample was homogenized in 700 μL of ice-cold buffer containing 70 mM sucrose, 210 mM mannitol, 5 mM HEPES, 1 mM ethylenediaminetetraacetic acid (EDTA), and protease and phosphatase inhibitors. Homogenates were incubated on ice for 30 min, followed by centrifugation at 800× *g* for 10 min at 4°C. Collected supernatant 1 was centrifuged at 10,000× *g* for 10 min at 4°C to obtain cytoplasmic fraction (supernatant 2) and a mitochondrial pellet.

Mitochondrial protein was obtained by resuspending mitochondrial pellets in ice-cold buffer containing 50 mM Tris, pH 8.0, 1 mM EDTA, 150 mM NaCl, and protease and phosphatase inhibitors, followed by sonication. After incubation on ice for 30 min, homogenates were centrifuged at 13,000× *g* for 15 min at 4°C, and the supernatant was used as mitochondrial protein. Protein concentration was measured using Bradford assay, according to manufacturer's instructions.

Western Blot Analysis

Proteins (35 μg total protein per sample) were separated on 10% sodium dodecyl sulfate polyacrylamide gel electrophoresis (SDS-PAGE) gel and transferred onto polyvinylidene fluoride membranes (Millipore). Membranes were blocked with 5% nonfat dry milk in 0.1% Tween-PBS (TBST) for 1 h at room temperature and incubated overnight at 4°C with primary antibodies against p53 (1:500; Cell Signaling Technology, Inc., Danvers, MA), HSP70 (1:500; Santa Cruz Biotechnology, Inc., Dallas, TX), cytochrome-c oxidoreductase (COX-IV) (1:1000, Invitrogen/Thermo Fisher Scientific), cleaved caspase-3 (1:1000, Cell Signaling Technology, Inc.), cytochrome-c (1:1000, BD Biosciences, San Jose, CA), Histone H1 (1:800, Abcam, Cambridge, MA) and HRP-conjugated mouse anti-β-actin (1:5000, Sigma-Aldrich, St. Louis, MO) in 5% bovine serum albumin/TBST. Membranes were

washed in TBST and then incubated with horseradish peroxidase (HRP)-conjugated secondary antibodies, either mouse immunoglobulin (Ig)G or rabbit IgG (Jackson ImmunoResearch, West Grove, PA) (1:5000 in 5% nonfat dry milk/TBST). HRP-conjugated mouse B-actin (Sigma-Aldrich) was incubated for 1 h at room temperature, washed, and developed. Specific bands were detected with Amersham ECL Western Blotting Detection Reagent (GE Healthcare Bio-Sciences, Pittsburgh, PA) and captured in the LAS system using Image Quant software for quantification of bands.

Statistics

All data are presented as mean ± standard error of the mean (SEM). Data were analyzed using GraphPad Prism 6 (GraphPad). One-way or two-way analysis of variance (ANOVA) was used with or without repeated measure to test for statistical significance where applicable. *Post hoc* pair-wise, multiple-comparisons were performed using the Tukey's test when needed. Differences were considered statistically significant at $P < 0.05$.

RESULTS

Effect of PFT-μ on Cisplatin-Induced Cognitive Impairment

Cisplatin (2.3 mg/kg) or phosphate-buffered saline (PBS) was administered i.p. daily for 5 days, followed by a 5-day rest period and another 5-day cycle of cisplatin. To investigate the effects of PFT-μ on cognitive function, PFT-μ (8 mg/kg) or vehicle was administered i.p. 1 h prior to cisplatin. The data presented in Figs. 1A and 1C demonstrate that performance in the NOPR and Y-maze tests was impaired in cisplatin-treated mice, whereas co-administration of PFT-μ prevented CICI completely. No differences were observed in the total time the animals interacted with objects in the NOPR, indicating that cisplatin had no effect on interest in the objects or on locomotor activity (Fig. 1B). Consistently, locomotor activity in the home cage was not affected by cisplatin (Fig. 1D). PFT-μ treatment did not prevent cisplatin-induced loss of body weight (Fig. 1E). Cisplatin (in the presence or absence of PFT-μ) did not induce depressive-like behavior in comparison with PBS-treated animals, as analyzed by sucrose preference (saline: 88.1 ± 1.4%; Cisplatin: 90.9 ± 1.3%) and forced-swim tests (saline: 55.2 ± 8.4 s; Cisplatin: 50.7 ± 11.9 s).

Effect of Cisplatin and PFT-μ on Neuronal Precursors in the Brain

The results in Fig. 2 show that our regimen of cisplatin treatment led to a decrease in the number of DCX^+ neural progenitors in the two major neurogenic niches in the brain. After 2 cycles of cisplatin, the number of DCX^+ neuroblasts in the DG of the hippocampus decreased by 70% (Figs. 2A–2E). The number of DCX^+ cells in the SVZ decreased by 30% (Figs. 2F–2I). Preventive treatment with PFT-μ completely prevented the loss of DCX^+ neuroblasts in both the DG and SVZ (Figs. 2D, I).

Effect of PFT-μ on Cisplatin-Induced Changes in White-Matter Integrity

As shown in Figs. 3A–3E, the two 5-day cycles of cisplatin used in the present study increased white-matter coherency, suggesting a loss of arborization and lateral fibers. The latter assumption is supported by the skeletonized MBP^+ structures shown in Figs. 3A'–3D'. Co-administration of PFT-μ prevented the cisplatin-induced increase in white-matter

coherency in the cingulate cortex (Figs. 3D and 3D'), implying that PFT-μ protects against structural white-matter damage induced by cisplatin.

Effect of Cisplatin on the Inflammatory Response in the Brain

In our analysis of the effect of cisplatin on the expression of IL-1β, IL-6, and TNF-α, GFAP, and CD11b, we did not detect any significant increase in cytokine mRNA after cisplatin treatment, as measured 24 h after the first injection or after the behavioral testing 1 week after the last dose of cisplatin (Table 1). Taken together, these data indicate that CICI in our mouse model is not associated with typical (neuro)inflammation.

Early Effects of Cisplatin and PFT-μ on p53 Translocation to Mitochondria and Caspase-3 Activation

Fig. 4A shows that the protein level of p53 in isolated brain mitochondrial fractions was increased at 4 h and 24 h after a single dose of cisplatin, as determined by Western blotting. Co-administration of PFT-μ completely prevented this cisplatin-induced increase in brain mitochondrial p53 (Fig. 4B). Cisplatin treatment did not lead to an increase in brain cytosolic cytochrome-c nor to activation of caspase-3 (Fig. 4C). The results in figure 4D confirm the purity of the subcellular fractions and show that there was no effect of cisplatin on cytosolic/nuclear p53. We did not detect changes in brain HSP70 after cisplatin treatment (Fig. 4E).

Effects of Cisplatin and PFT-μ on Mitochondrial Morphology and Mitochondrial Function

The results in Figs. 5A–5F demonstrate that synaptosomal mitochondria of brains of cisplatin-treated animals were swollen and had abnormal cristae when compared with synaptosomal mitochondria from PBS-treated control mice. PFT-μ co-administration prevented this long-lasting abnormal morphology of the mitochondria induced by two cycles of cisplatin (Figs. 5D–5F).

Basal respiration of the synaptosomes was not affected by cisplatin (Fig. 5G), and there was no effect of cisplatin on the oxygen consumption related to ATP production (Fig. 5H). However, the maximal respiration as determined after addition of the mitochondrial uncoupler FCCP was significantly lower in synaptosomal fractions of cisplatin-treated mice versus PBS-treated control mice (Fig. 5I). Consequently, the difference between maximal and basal respiration, also known as spare respiratory capacity, was decreased in the synaptosomes from cisplatin-treated mice (Fig. 5J). Co-administration of PFT-μ prevented the cisplatin-induced impairment in maximal and spare respiratory capacity (Figs. 5G–5J). No differences in proton leak between cisplatin-treated and PBS-treated mice were observed (saline: 0.28 ± 0.01 pmol O_2/μg of Protein; Cisplatin 0.33 ± 0.11 pmol O_2/μg of Protein). We did not detect cisplatin-induced changes in lipid peroxidation as quantified using a TBARS assay (saline: 4.32 ± 0.24 nM/μg total protein; Cisplatin: 4.39 ± 0.38 nM/μg total protein)

Effect of PFT-μ on the Sensitivity of the Tumor to Chemoradiation

We used a heterotopic syngeneic murine model of human papilloma virus (HPV)-related head and neck cancer to assess whether PFT-μ might potentially interfere with the tumor's

response to chemoradiation (cisplatin + radiation CRT). CRT inhibited tumor growth as expected (Fig. 6A). The response to CRT was not adversely affected by PFT-μ treatment. Further, the addition of PFT-μ to the cancer treatment did not significantly influence body-weight loss (Fig. 6B).

DISCUSSION

We show for the first time that the inhibitor of mitochondrial p53 accumulation, PFT-μ, prevented cisplatin-induced cognitive impairment or “chemobrain” in mice, as assessed in the NOPR and Y-maze tests (Figs. 1A, 1C). The impaired cognitive function observed in cisplatin-treated mice was associated with impaired cerebral neurogenesis (Fig. 2) and structural abnormalities in cerebral white matter that were prevented by PFT-μ (Fig. 3). Mechanistically, we show that cisplatin increased brain mitochondrial p53 levels (Fig. 4) and induced abnormal mitochondrial morphology and impaired the spare respiratory capacity of synaptosomal mitochondria, as shown by Seahorse analysis (Fig. 5). Notably, PFT-μ prevented not only the functional and structural abnormalities induced by cisplatin, but also the cisplatin-induced increase in mitochondrial p53 and the abnormalities in brain mitochondrial function and morphology.

Although (neuro)inflammation has often been proposed as a mechanism for chemotherapy-induced neurotoxicities, we did not find evidence for increased cytokine production in the brains of cisplatin-treated mice 24 h or 1 week after the last injection of cisplatin (Table1). In line with these results, we also did not detect microglial or astrocyte activation, as analyzed by Iba-1 and GFAP fluorescence, nor a change in the morphological appearance of microglia and astrocytes. Therefore, we suggest that neuroinflammation does not play a major role in CICI. We cannot exclude, however, the possibility of limited region-specific inflammation and/or short-lasting inflammation at other time points.

Interestingly, our current data point toward a key role for damage to brain mitochondria as the mechanism underlying CICI. It has been shown that cisplatin-induced peripheral neuropathy is associated with changes in mitochondrial morphology in peripheral sensory neurons [3], [13]. However, to the best of our knowledge, we are the first to show that systemic administration of cisplatin induces structural changes in synaptosomal mitochondria (Fig. 5A–5F). This abnormal morphology is associated with a decrease in mitochondrial bioenergetic function, as reflected by a lower spare respiratory capacity in cerebral synaptosomes of cisplatin-treated mice (Fig. 5G–5J). Spare respiratory capacity is viewed as an index of mitochondrial health and is a measure of how well a cell can produce energy under stressful energy-demanding conditions [13], [34]. Notably, there is evidence that decreased spare respiratory capacity is associated with cognitive impairment in rodent models of Alzheimer disease [33].

In support of our hypothesis that mitochondrial dysfunction is a central mechanism of CICI, we show here that treatment with PFT-μ which prevents mitochondrial p53 translocation prevented the reduction in synaptosomal mitochondrial spare respiratory capacity as well as the behavioral deficits, implying a causal relation between mitochondrial protection and CICI. It remains to be determined whether this reduction in spare respiratory capacity in

response to cisplatin reflects a general deficit in all mitochondria in the brain or if it is specific for mitochondria in the synapses. The relatively high mitochondrial density in nerve terminals might render this cellular compartment most sensitive to cellular stress [34]. A decrease in mitochondrial function and spare respiratory capacity has also been associated with decreased cognitive ability in Alzheimer's disease [35] and aging [36], [37]. In this respect, it is of interest that advanced neuroimaging has shown that in cancer patients, the severity of cognitive impairment is analogous to multiple years of brain aging [38].

Strom et al. originally identified PFT-μ as a compound that inhibits accumulation of p53 at the mitochondria without inhibiting p53 transcriptional activity [39]. These authors showed that PFT-μ inhibits radiation-induced p53-dependent thymocyte apoptosis *in vitro* and *in vivo*. PFT-μ was proposed to protect against apoptosis by reducing the binding of p53 to both Bcl-xL and Bcl-2, resulting in preservation of mitochondrial integrity [39].

We previously investigated the protective effects of PFT-μ in a model of neonatal hypoxic–ischemic (HI) brain damage. PFT-μ was shown to prevent HI-induced loss of white- and gray-matter and to preserve behavioral features like motoric and cognitive function [15]. Mechanistically, HI was shown to increase early neuronal p53 mitochondrial accumulation, reactive oxygen species, and cytosolic accumulation of pro-apoptotic proteins, as measured by increased cytosolic cytochrome-c and activated caspase-3 levels [32]. Here we show that administration of cisplatin rapidly increased mitochondrial levels of p53, which was prevented by co-administration of PFT-μ (Figs. 4A, 4B). However, the increase in mitochondrial p53 as a result of cisplatin treatment did not initiate a general apoptotic cascade, because neither cytosolic cytochrome-c nor activated caspase-3 were increased either at 4 h or 24 h after cisplatin treatment (Fig. 4C). The absence of apoptosis may have been caused by the fact that cisplatin does not induce early nuclear factor-κB activation and subsequent cytokine synthesis, as was seen early after HI brain damage at the moment of mitochondrial p53 accumulation [32]. However, we did observe structural changes and functional mitochondrial impairment after cisplatin treatment, all of which were prevented by PFT-μ (Figs. 5). Cisplatin treatment did not lead to increases in cytosolic p53. Moreover, as already shown by Strom et al.[39], PFT-μ did not interfere with cytosolic p53 levels.

Therefore, we propose that the cisplatin-induced increase in mitochondrial p53 reduces synaptosomal mitochondrial integrity, possibly by decreasing mitochondrial membrane potential [40] and thereby decreasing the availability of cellular energy under demanding conditions, which may result in oxidative cellular damage in neuronal circuitries engaged in cognition.

At the level of brain structure, we observed cisplatin-induced abnormalities in white-matter structure in the cingulum that were also prevented by PFT-μ (Fig. 3). Moreover, we recently showed that cisplatin reduces arborization and spine density of pyramidal neurons in the cingulum [2]. Van Schependom et al. described that neural disconnections, especially of white-matter tracts connecting both hemispheres seen in cognitively impaired versus cognitively preserved patients with multiple sclerosis, were responsible for the cognitive impairment observed in these patients [41]. Diffusion tensor neuroimaging of the brains of lung cancer patients indicates that cisplatin treatment results in an increased fractional

anisotropy in areas of white matter in the cingulate cortex. Kesler et al. recently published advanced neuroimaging data of patients treated with the anthracycline doxorubicin and concluded that lower memory performance was associated with decreased functional and structural connectivity [38], [42]. In line with these findings, we demonstrate here in mice that cisplatin treatment resulted in increased overall coherency of white-matter fibers in the cingulum, a feature underlying the changes in fractional anisotropy in patients, which may contribute to the observed cognitive impairment. We do not have evidence for an overall decrease in intensity or area of MBP staining, indicating that the major fibers are not lost. Therefore, we conclude that cisplatin treatment leads to a loss of MBP positive branches rather than an overall loss of MBP+ tissue. In a previous study we showed that cisplatin treatment reduces dendritic branching as assessed at the individual neuron level using Golgi staining to visualize dendrites [2]. It is likely that the reduction in the complexity of the organization of MBP-staining in the same area is a consequence of the loss of dendritic complexity in response to cisplatin. If so, it is likely that the primary damage is caused by increased p53 binding to neuronal mitochondria, leading to mitochondrial insufficiency, dendritic damage and subsequent loss of MBP positive small fibers. However, it is possible that there is a direct effect of cisplatin on mitochondria in oligodendrocytes that could contribute to abnormal pattern of MBP staining in cisplatin-treated mice. For example, it has been shown that cisplatin reduces survival of oligodendrocytes *in vitro* and *in vivo* [43]. Therefore, we cannot exclude that in vivo PFT-μ prevents the mitochondrial accumulation of p53 in oligodendrocytes as well.

Although we do not have evidence for global activation of apoptotic pathways after cisplatin treatment, we cannot exclude that a limited number of cells, such as proliferating cells in the stem cell compartment, undergo apoptotic cell death.

Adult neurogenesis is required for integration of circuitry during learning and memory, as reviewed by Deng et al. and the sharp decrease in DCX^+ cells in the neurogenic niches induced by cisplatin may well contribute to the observed cognitive deficits [27]. Interestingly, the decrease in the number of DCX^+ neuroblasts as a result of cisplatin treatment was also completely prevented by PFT-μ (Fig. 2). Preliminary data indicate that the number of uncommitted $Nestin^+$ $GFAP^+$ stem cells in the SVZ did not change under influence of cisplatin, which might indicate that cisplatin selectively affects migrating proliferating neuroblasts (DCX^+) and/or that the differentiation of uncommitted stem cells to neuroblasts is arrested possibly in favor of glial cells. In this respect, the study of Wang et al., which showed that oxidative damage to mitochondrial DNA in neural stem cells inhibits neural stem cell differentiation and represents a primary signal for elevated astrogliosis, is of interest [44]. Because cisplatin has been shown to damage mtDNA in neurons [45], the sharp decrease in DCX^+ cells may well be a reflection of the relatively high sensitivity of neural stem cells for oxidative damage to mtDNA, in comparison with adult neurons. These data may also imply that the differentiation of the neural progenitors is inhibited in favor of glial differentiation.

On the basis of our current data, we propose that mitochondrial protectants may represent an attractive, efficacious treatment for chemotherapy-induced neurotoxicities. It remains to be determined whether the observed reduction in neuronal precursors and the white matter

abnormalities are a direct consequence of mitochondrial abnormalities in the synaptosomes or are due to effects of cisplatin on the neuronal stem cells and oligodendrocytes themselves. We recently showed that PFT-μ also prevents taxane-induced and cisplatin-induced peripheral neuropathy[3]. Emerging data suggest that PFT-μ acts as an anti-cancer agent [30], [46]–[48]. Consistently, we show here *in vivo* that PFT-μ does not interfere with the anti-tumor efficacy of a cisplatin-based chemoradiation regimen in a heterotopic murine model of HPV-related head and neck cancer. Mechanistically, it has been shown that PFT-μ promotes tumor-cell death *in vitro* and *in vivo* via an autophagy-promoting mechanism involving interaction with the stress protein HSP70 and lysosome-associated membrane protein 2 in rapidly proliferating tumor cells [30], [31], [46], [48], [49]. These effects of PFT-μ on tumor cells are independent of p53.

Taken together, our results indicate that systemic administration of a mitochondrial protectant such as PFT-μ may not only be capable of protecting against peripheral and central neurotoxicities, but also will act as an adjuvant therapy to promote tumor cell death without interfering with the efficacy of the cancer therapy. We propose that prevention of mitochondrial p53 accumulation due to chemotherapy is an important therapeutic target to prevent cancer treatment-induced peripheral and central neurotoxicities. The addition of PFT-μ to cisplatin may well represent a promising novel therapeutic approach to help fight tumor growth and the development of neurotoxicities in patients with cancer.

Acknowledgments

The authors are greatly indebted to Dr. Kathy Mason and Jessica M. Molkentine for performing the CRT on mice with the heterotopic HPV-tumor. We thank Dr. John Lee (Sanford Research) for providing the MEER cell line for the tumor model. Processing for electron microscopy was performed by Kenneth Dunner Jr. at the High Resolution Electron Microscopy Facility at MD Anderson Cancer Center. We thank Jason Lu and Siddiqua Noor for quantification of DCX^+ staining and quantification of mitochondrial morphology.

The authors acknowledge the editorial assistance of Jeanie F. Woodruff, BS, ELS.

Financial Support: This research was funded by grants from the National Institutes of Health (R21 CA183736 to C.J. Heijnen and R. Dantzer, R01 CA193522 to R. Dantzer, and MD Anderson Cancer Center Support Grant P30 CA016672, which supports the institution's High Resolution Electron Microscopy Facility) and from The University of Texas MD Anderson Cancer Center (the Institutional Research Grant Program and the Knowledge Gap Chemobrain Project of the Moon Shots Program).

REFERENCES

1. de Moor JS, Mariotto AB, Parry C, Alfano CM, Padgett L, Kent EE, Forsythe L, Scoppa S, Hachey M, Rowland JH. Cancer survivors in the United States: prevalence across the survivorship trajectory and implications for care. Cancer Epidemiol. Biomarkers Prev. 2013 Apr; 22(4):561–570. [PubMed: 23535024]
2. Zhou W, Kavelaars A, Heijnen CJ. Metformin Prevents Cisplatin-Induced Cognitive Impairment and Brain Damage in Mice. PLoS One. 2016 Mar.11(3):e0151890. [PubMed: 27018597]
3. Krukowski K, Nijboer CH, Huo X, Kavelaars A, Heijnen CJ. Prevention of chemotherapy-induced peripheral neuropathy by the small-molecule inhibitor pifithrin-[mu]. Pain. 2015; 156(11):2184–2192. [PubMed: 26473292]
4. Vichaya EG, Chiu GS, Krukowski K, Lacourt TE, Kavelaars A, Dantzer R, Heijnen CJ, Walker AK. Mechanisms of chemotherapy-induced behavioral toxicities. Front. Neurosci. 2015 Jan.9:131. [PubMed: 25954147]

5. Simó M, Rifà-Ros X, Rodriguez-Fornells A, Bruna J. Chemobrain: a systematic review of structural and functional neuroimaging studies. Neurosci. Biobehav. Rev. 2013 Sep; 37(8):1311–1321. [PubMed: 23660455]
6. Wang X-M, Walitt B, Saligan L, Tiwari AF, Cheung CW, Zhang Z-J. Chemobrain: A critical review and causal hypothesis of link between cytokines and epigenetic reprogramming associated with chemotherapy. Cytokine. 2015 Mar; 72(1):86–96. [PubMed: 25573802]
7. Wefel JS, Schagen SB. Chemotherapy-related cognitive dysfunction. Curr. Neurol. Neurosci. Rep. 2012 Jun; 12(3):267–275. [PubMed: 22453825]
8. Deprez S, Amant F, Smeets A, Peeters R, Leemans A, Van Hecke W, Verhoeven JS, Christiaens M-R, Vandenberghe J, Vandenbulcke M, Sunaert S. Longitudinal assessment of chemotherapy-induced structural changes in cerebral white matter and its correlation with impaired cognitive functioning. J. Clin. Oncol. 2012 Jan; 30(3):274–281. [PubMed: 22184379]
9. Craig CD, Monk BJ, Farley JH, Chase DM. Cognitive impairment in gynecologic cancers: a systematic review of current approaches to diagnosis and treatment. Support. Care Cancer. 2014 Jan; 22(1):279–287. [PubMed: 24212261]
10. Al Moundhri MS, Al-Salam S, Al Mahrouqee A, Beegam S, Ali BH. The effect of curcumin on oxaliplatin and cisplatin neurotoxicity in rats: some behavioral, biochemical, and histopathological studies. J. Med. Toxicol. 2013 Mar; 9(1):25–33. [PubMed: 22648527]
11. Takahara PM, Rosenzweig AC, Frederick CA, Lippard SJ. Crystal structure of double-stranded DNA containing the major adduct of the anticancer drug cisplatin. Nature. 1995 Oct; 377(6550): 649–652. [PubMed: 7566180]
12. Seigers R, Schagen SB, Van Tellingen O, Dietrich J. Chemotherapy-related cognitive dysfunction: current animal studies and future directions. Brain Imaging Behav. 2013 Dec; 7(4):453–459. [PubMed: 23949877]
13. Zheng H, Xiao WH, Bennett GJ. Functional deficits in peripheral nerve mitochondria in rats with paclitaxel- and oxaliplatin-evoked painful peripheral neuropathy. Exp. Neurol. 2011 Dec; 232(2): 154–161. [PubMed: 21907196]
14. Mecocci P, MacGarvey U, Beal MF. Oxidative damage to mitochondrial DNA is increased in Alzheimer's disease. Ann. Neurol. 1994 Nov; 36(5):747–751. [PubMed: 7979220]
15. Nijboer CH, Heijnen CJ, van der Kooij MA, Zijlstra J, van Velthoven CTJ, Culmsee C, van Bel F, Hagberg H, Kavelaars A. Targeting the p53 pathway to protect the neonatal ischemic brain. Ann. Neurol. 2011 Aug; 70(2):255–264. [PubMed: 21674585]
16. Chiu GS, Chatterjee D, Darmody PT, Walsh JP, Meling DD, Johnson RW, Freund GG. Hypoxia/reoxygenation impairs memory formation via adenosine-dependent activation of caspase 1. J. Neurosci. 2012 Oct; 32(40):13945–13955. [PubMed: 23035103]
17. Kaczmarczyk MM, Machaj AS, Chiu GS, Lawson MA, Gainey SJ, York JM, Meling DD, Martin SA, Kwakwa KA, Newman AF, Woods JA, Kelley KW, Wang Y, Miller MJ, Freund GG. Methylphenidate prevents high-fat diet (HFD)-induced learning/memory impairment in juvenile mice. Psychoneuroendocrinology. 2013 Sep; 38(9):1553–1564. [PubMed: 23411461]
18. Chiu GS, Darmody PT, Walsh JP, Moon ML, Kwakwa KA, Bray JK, McCusker RH, Freund GG. Adenosine through the A2A adenosine receptor increases IL-1β in the brain contributing to anxiety. Brain. Behav. Immun. 2014 Oct.41:218–231. [PubMed: 24907587]
19. Moon ML, Joesting JJ, Lawson MA, Chiu GS, Blevins NA, Kwakwa KA, Freund GG. The saturated fatty acid, palmitic acid, induces anxiety-like behavior in mice. Metabolism. 2014 Sep; 63(9):1131–1140. [PubMed: 25016520]
20. Zhou W, Dantzer R, Budac DP, Walker AK, Mao-Ying Q-L, Lee AW, Heijnen CJ, Kavelaars A. Peripheral indoleamine 2,3-dioxygenase 1 is required for comorbid depression-like behavior but does not contribute to neuropathic pain in mice. Brain. Behav. Immun. 2015 May.46:147–153. [PubMed: 25637485]
21. Spanos WC, Hoover A, Harris GF, Wu S, Strand GL, Anderson ME, Klingelhutz AJ, Hendriks W, Bossler AD, Lee JH. The PDZ binding motif of human papillomavirus type 16 E6 induces PTPN13 loss, which allows anchorage-independent growth and synergizes with ras for invasive growth. J. Virol. 2008 Mar; 82(5):2493–2500. [PubMed: 18160445]

22. Spanos WC, Nowicki P, Lee DW, Hoover A, Hostager B, Gupta A, Anderson ME, Lee JH. Immune response during therapy with cisplatin or radiation for human papillomavirus-related head and neck cancer. Arch. Otolaryngol. Head. Neck Surg. 2009 Nov; 135(11):1137–1146. [PubMed: 19917928]

23. Vichaya EG, Molkentine JM, Vermeer DW, Walker AK, Feng R, Holder G, Luu K, Mason RM, Saligan L, Heijnen CJ, Kavelaars A, Mason KA, Lee JH, Dantzer R. Sickness behavior induced by cisplatin chemotherapy and radiotherapy in a murine head and neck cancer model is associated with altered mitochondrial gene expression. Behav. Brain Res. 2016 Jan.297:241–250. [PubMed: 26475509]

24. Kipnis J, Derecki NC, Yang C, Scrable H. Immunity and cognition: what do age-related dementia, HIV-dementia and 'chemo-brain' have in common? Trends Immunol. 2008 Oct; 29(10):455–463. [PubMed: 18789764]

25. Mills PJ, Parker B, Dimsdale JE, Sadler GR, Ancoli-Israel S. The relationship between fatigue and quality of life and inflammation during anthracycline-based chemotherapy in breast cancer. Biol. Psychol. 2005 Apr; 69(1):85–96. [PubMed: 15740827]

26. Ganz PA, Bower JE, Kwan L, Castellon SA, Silverman DHS, Geist C, Breen EC, Irwin MR, Cole SW. Does tumor necrosis factor-alpha (TNF-α) play a role in post-chemotherapy cerebral dysfunction? Brain. Behav. Immun. 2013 Mar; 30(Suppl):S99–S108. [PubMed: 22884417]

27. Zhao C, Deng W, Gage FH. Mechanisms and functional implications of adult neurogenesis. Cell. 2008 Feb; 132(4):645–660. [PubMed: 18295581]

28. Villeda SA, Luo J, Mosher KI, Zou B, Britschgi M, Bieri G, Stan TM, Fainberg N, Ding Z, Eggel A, Lucin KM, Czirr E, Park J-S, Couillard-Després S, Aigner L, Li G, Peskind ER, Kaye JA, Quinn JF, Galasko DR, Xie XS, Rando TA, Wyss-Coray T. The ageing systemic milieu negatively regulates neurogenesis and cognitive function. Nature. 2011 Sep; 477(7362):90–94. [PubMed: 21886162]

29. Kamat PK, Kalani A, Tyagi N. Method and validation of synaptosomal preparation for isolation of synaptic membrane proteins from rat brain. MethodsX. 2014 Jan; 1(2014):102–107. [PubMed: 25250220]

30. Monma H, Harashima N, Inao T, Okano S, Tajima Y, Harada M. The HSP70 and autophagy inhibitor pifithrin-μ enhances the antitumor effects of TRAIL on human pancreatic cancer. Mol. Cancer Ther. 2013 Apr; 12(4):341–351. [PubMed: 23371857]

31. Leu JI-J, Pimkina J, Frank A, Murphy ME, George DL. A small molecule inhibitor of inducible heat shock protein 70. Mol. Cell. 2009 Oct; 36(1):15–27. [PubMed: 19818706]

32. Nijboer CH, Heijnen CJ, van der Kooij MA, Zijlstra J, van Velthoven CTJ, Culmsee C, van Bel F, Hagberg H, Kavelaars A. Targeting the p53 pathway to protect the neonatal ischemic brain. Ann. Neurol. 2011 Aug; 70(2):255–264. [PubMed: 21674585]

33. Kennedy MA, Moffat TC, Gable K, Ganesan S, Niewola-Staszkowska K, Johnston A, Nislow C, Giaever G, Harris LJ, Loewith R, Zaremberg V, Harper ME, Dunn T, Bennett SA, Baetz K. A Signaling Lipid Associated with Alzheimer's Disease Promotes Mitochondrial Dysfunction. Sci Rep. 2016; 6:19332. [PubMed: 26757638]

34. Miltenburg NC, Boogerd W. Chemotherapy-induced neuropathy: A comprehensive survey. Cancer Treatment Reviews. 2014; 40(7):872–882. [PubMed: 24830939]

35. Reddy PH, Beal MF. Amyloid beta, mitochondrial dysfunction and synaptic damage: implications for cognitive decline in aging and Alzheimer's disease. Trends Mol. Med. 2008 Feb; 14(2):45–53. [PubMed: 18218341]

36. Bishop NA, Lu T, Yankner BA. Neural mechanisms of ageing and cognitive decline. Nature. 2010 Mar; 464(7288):529–535. [PubMed: 20336135]

37. Liu J, Head E, Gharib AM, Yuan W, Ingersoll RT, Hagen TM, Cotman CW, Ames BN. Memory loss in old rats is associated with brain mitochondrial decay and RNA/DNA oxidation: partial reversal by feeding acetyl-L-carnitine and/or R-alpha -lipoic acid. Proc. Natl. Acad. Sci. U. S. A. 2002 Feb; 99(4):2356–2361. [PubMed: 11854529]

38. Kesler SR, Blayney DW. Neurotoxic Effects of Anthracycline- vs Nonanthracycline-Based Chemotherapy on Cognition in Breast Cancer Survivors. JAMA Oncol. 2016 Feb; 2(2):185–192. [PubMed: 26633037]

39. Strom E, Sathe S, Komarov PG, Chernova OB, Pavlovska I, Shyshynova I, Bosykh DA, Burdelya LG, Macklis RM, Skaliter R, Komarova EA, Gudkov AV. Small-molecule inhibitor of p53 binding to mitochondria protects mice from gamma radiation. Nat. Chem. Biol. 2006 Sep; 2(9):474–479. [PubMed: 16862141]
40. Li P, Dietz R, van Harsdorf R. p53 regulates mitochondrial membrane potential through reactive oxygen species and induces cytochrome c -independent apoptosis blocked by Bcl-2. EMBO J. 1999 Nov; 18(21):6027–6036. [PubMed: 10545114]
41. Van Schependom J, Gielen J, Laton J, D'hooghe MB, De Keyser J, Nagels G. Graph theoretical analysis indicates cognitive impairment in MS stems from neural disconnection. NeuroImage. Clin. 2014 Jan.4:403–410. [PubMed: 24567912]
42. Kesler S, Janelsins M, Koovakkattu D, Palesh O, Mustian K, Morrow G, Dhabhar FS. Reduced hippocampal volume and verbal memory performance associated with interleukin-6 and tumor necrosis factor-alpha levels in chemotherapy-treated breast cancer survivors. Brain. Behav. Immun. 2013 Mar; 30(Suppl):S109–S116. [PubMed: 22698992]
43. Dietrich J, Han R, Yang Y, Mayer-Pröschel M, Noble M. CNS progenitor cells and oligodendrocytes are targets of chemotherapeutic agents in vitro and in vivo. J. Biol. 2006; 5(7): 22. [PubMed: 17125495]
44. Wang W, Esbensen Y, Kunke D, Suganthan R, Rachek L, Bjørås M, Eide L. Mitochondrial DNA damage level determines neural stem cell differentiation fate. J. Neurosci. 2011 Jun; 31(26):9746–9751. [PubMed: 21715639]
45. Podratz JL, Knight AM, Ta LE, Staff NP, Gass JM, Genelin K, Schlattau A, Lathroum L, Windebank AJ. Cisplatin induced Mitochondrial DNA damage in dorsal root ganglion neurons. Neurobiol. Dis. 2011; 41(3):661–668. [PubMed: 21145397]
46. Kaiser M, Kühnl A, Reins J, Fischer S, Ortiz-Tanchez J, Schlee C, Mochmann LH, Heesch S, Benlasfer O, Hofmann W-K, Thiel E, Baldus CD. Antileukemic activity of the HSP70 inhibitor pifithrin-μ in acute leukemia. Blood Cancer J. 2011 Jul.1(7):e28. [PubMed: 22829184]
47. Ma L, Sato F, Sato R, Matsubara T, Hirai K, Yamasaki M, Shin T, Shimada T, Nomura T, Mori K, Sumino Y, Mimata H. Dual targeting of heat shock proteins 90 and 70 promotes cell death and enhances the anticancer effect of chemotherapeutic agents in bladder cancer. Oncol. Rep. 2014; 31(6):2482–2492. [PubMed: 24718854]
48. Sekihara K, Harashima N, Tongu M, Tamaki Y, Uchida N, Inomata T, Harada M. Pifithrin-μ, an inhibitor of heat-shock protein 70, can increase the antitumor effects of hyperthermia against human prostate cancer cells. PLoS One. 2013 Nov.8(11):e78772. [PubMed: 24244355]
49. Nanbu K, Konishi I, Mandai M, Kuroda H, Hamid AA, Komatsu T, Mori T. Prognostic Significance of Heat Shock Proteins HSP70 and HSP90 in Endometrial Carcinomas. Cancer Detect. Prev. 1998 Nov; 22(6):549–555. [PubMed: 9824379]

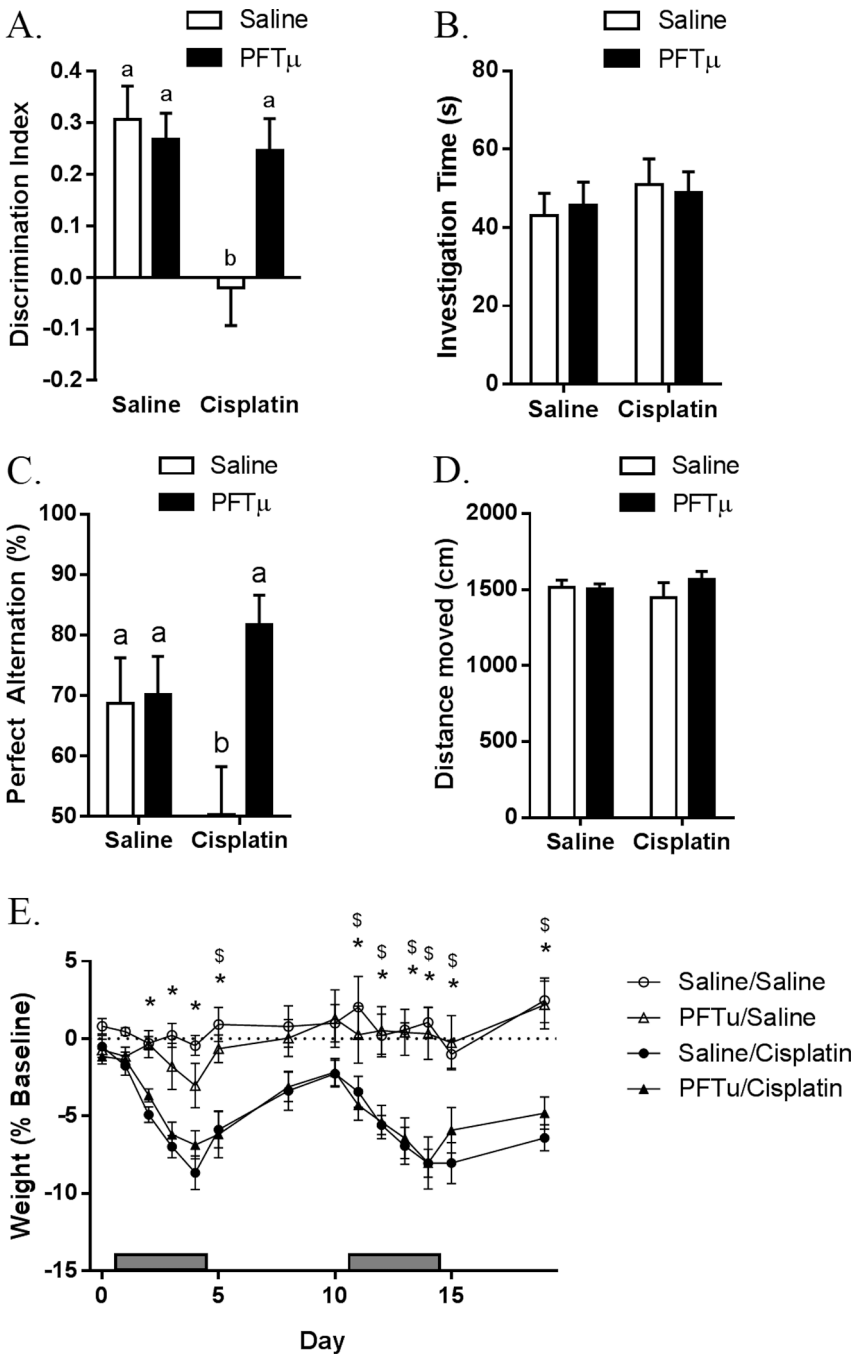

Figure 1. Effect of PFT-μ on cisplatin-induced cognitive impairment

Animals were treated with cisplatin and PFT-μ for two 5-day cycles. (**A**) NOPR was performed 7 days after the last injection, and discrimination index was calculated. (**B**) Total investigation time between both objects in the NOPR was recorded. Results are expressed as means ± SEM; n = 8. Bars without a common superscript are significantly different ($P < 0.05$). (**C**) Y-maze was performed 7 days after the last injection, and percentage of perfect alternation was calculated. Results are expressed as means ± SEM; n = 4. Bars without a common superscript are significantly different ($P < 0.05$). (**D**) Spontaneous locomotor

activity (total distance traveled) was measured. Results are expressed as means ± SEM; n = 8. (**E**) Percentage of baseline body weight was recorded. Results are expressed as means ± SEM; n = 12. *$P < 0.05$ saline/PBS vs. saline/cisplatin, $P < 0.05$ PFT-μ/PBS vs. PFT-μ/cisplatin.

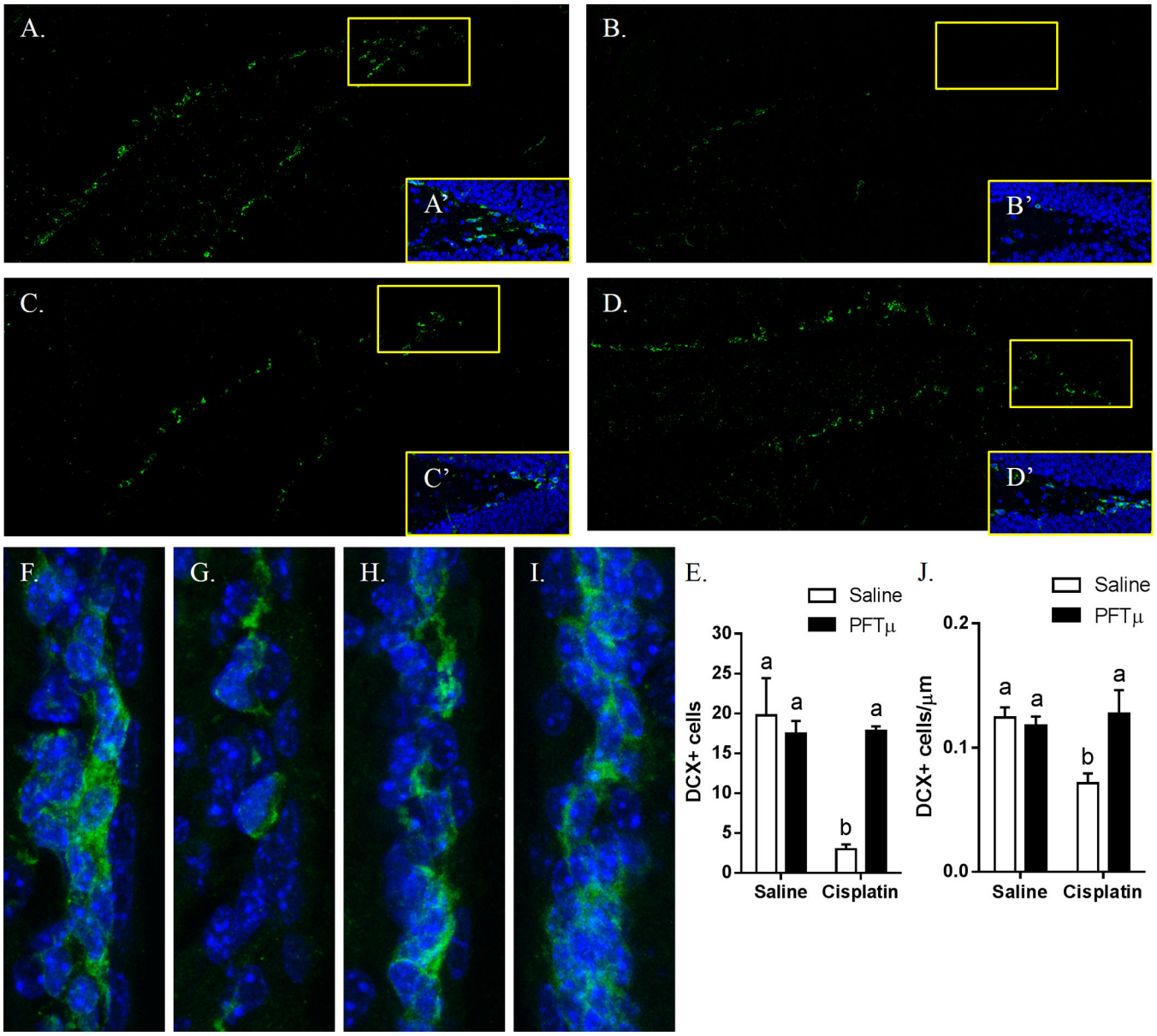

Figure 2. Effect of cisplatin and PFT-μ on neuronal precursors cells in the brain

Animals were treated with cisplatin and PFT-μ for two 5-day cycles. **(A, F)** PBS-treated animals. **(B, G)** Cisplatin-treated animals. **(C, H)** PFT-μ–treated animals. **(D, I)** PFT-μ/cisplatin-treated animals. DCX^+ neuronal precursors were observed in the **(A–D)** DG of the hippocampus and **(F–I)** SVZ. **(A'–D')** 40× magnification of the DG tip. DCX^+ cells were counted in the **(E)** DG and the **(J)** SVZ.

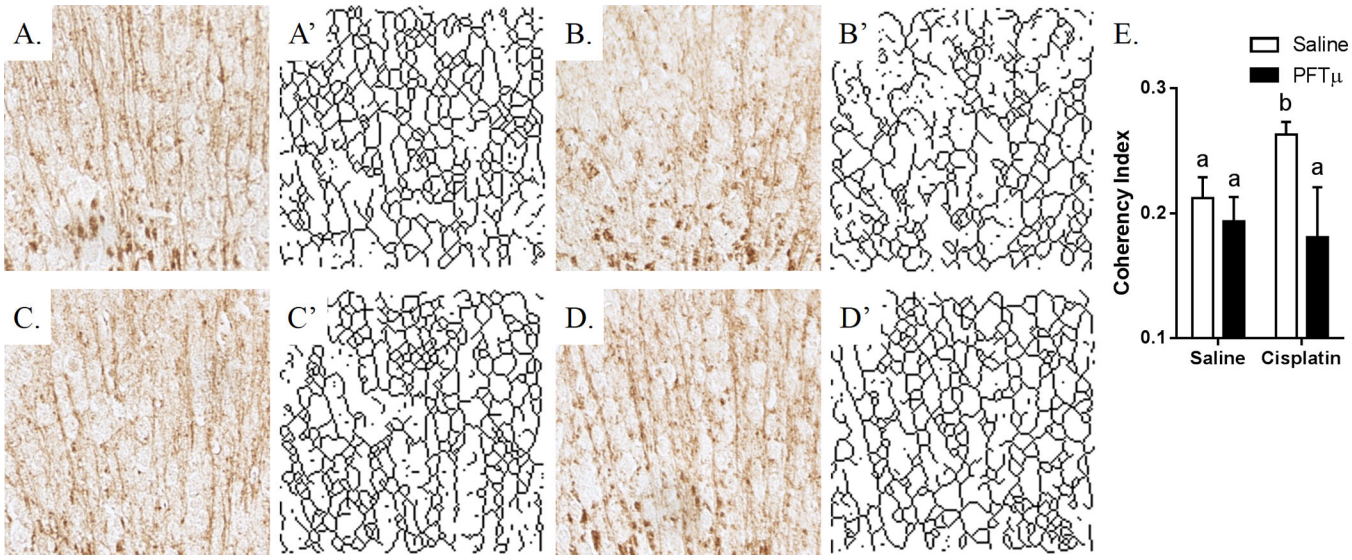

Figure 3. Effect of cisplatin and PFT-μ on white-matter coherency in the brain

Animals were treated with cisplatin and PFT-μ for two 5-day cycles. **(A)** PBS-treated animals. **(B)** Cisplatin-treated animals. **(C)** PFT-μ–treated animals. **(D)** PFT-μ/cisplatin-treated animals. **(A–D)** MBP staining was performed at the cingulum of the brain. **(A'–D')** Skeletonized display of the MBP staining. **(E)** Coherency index was calculated using ImageJ with the OrientationJ Plugin. Skeletonized structures were created using ImageJ by converting the sample image to a binary 8-bit image and then processed with the Skeletonize (2D/3D) Plugin.

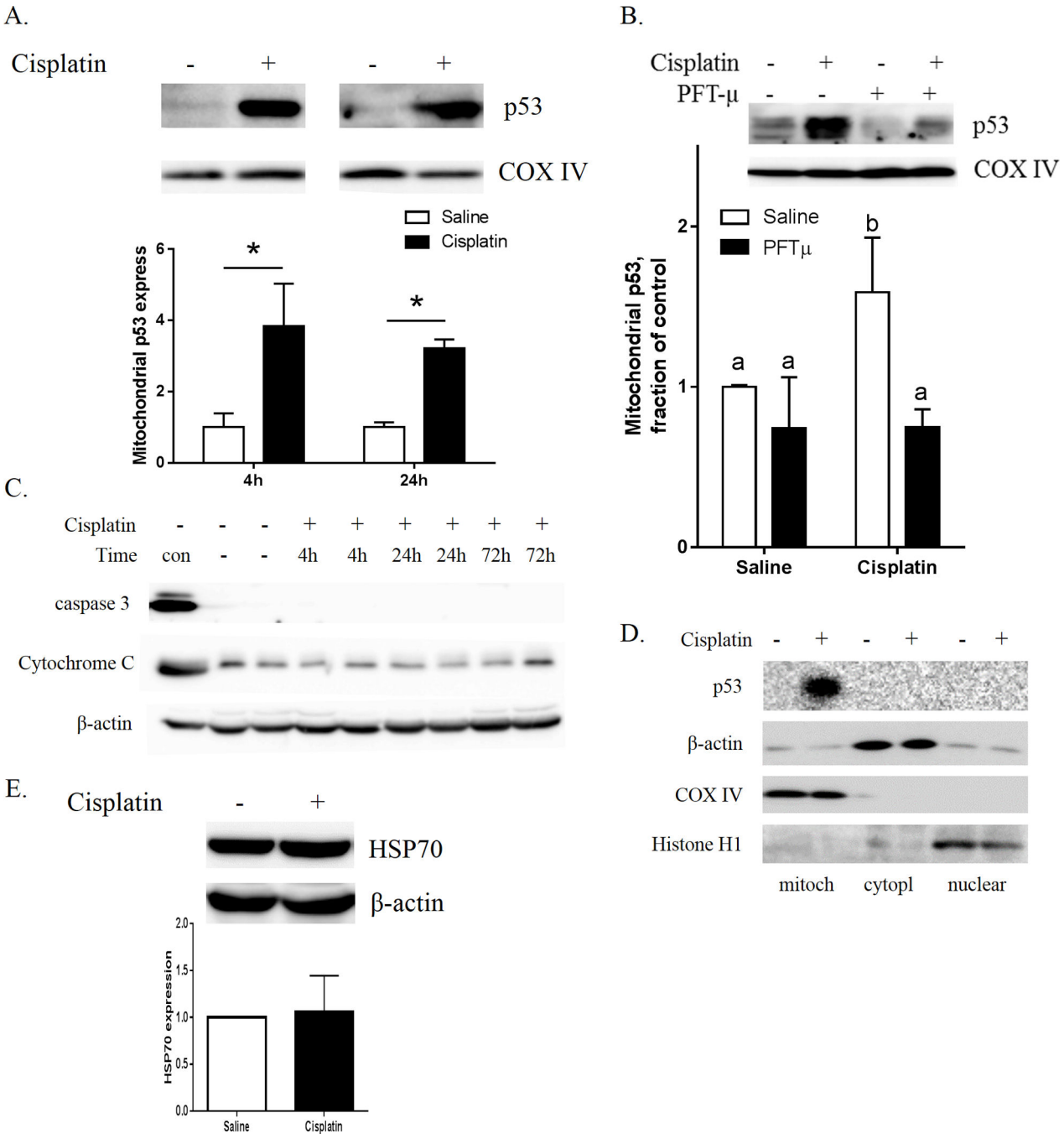

Figure 4. Acute effects of cisplatin on p53 translocation to the mitochondria and caspase-3 activation

(A) Mitochondrial p53 was measured 4 h and 24 h after cisplatin injection and **(B)** 4 h after cisplatin and PFT-μ injections. COX-IV was used as a protein loading control. Relative expression of p53 was calculated 4 h and 24 h after cisplatin treatment. **(C)** The cytosolic fractions were analyzed for the apoptotic markers cytochrome-c and cleaved caspase-3 4 h, 24 h, and 72 h after a single dose of cisplatin. "Con" designates positive controls: brain mitochondria fraction for cytochrome-c (upper panel), and whole-cell lysate of H_2O_2-treated

N2A cells for active caspase-3 (middle panel). β-actin was used as a protein loading control for cytosolic proteins. **(D.)** Cisplatin increases mitochondrial p53 without inducing p53 in cytosol or nucleus. Subcellular fractions collected at 4 h after cisplatin injection were analyzed for p53, Cox-IV (mitochondria), β-actin (cytosol and mitochondria) and Histone H1 (nuclear fraction). **(E)** Cytosolic HSP70. β-actin was used as a protein loading control. Results are expressed as means ± SEM; n = 6. *$P < 0.05$. Bars without a common superscript are significantly different ($P < 0.05$).

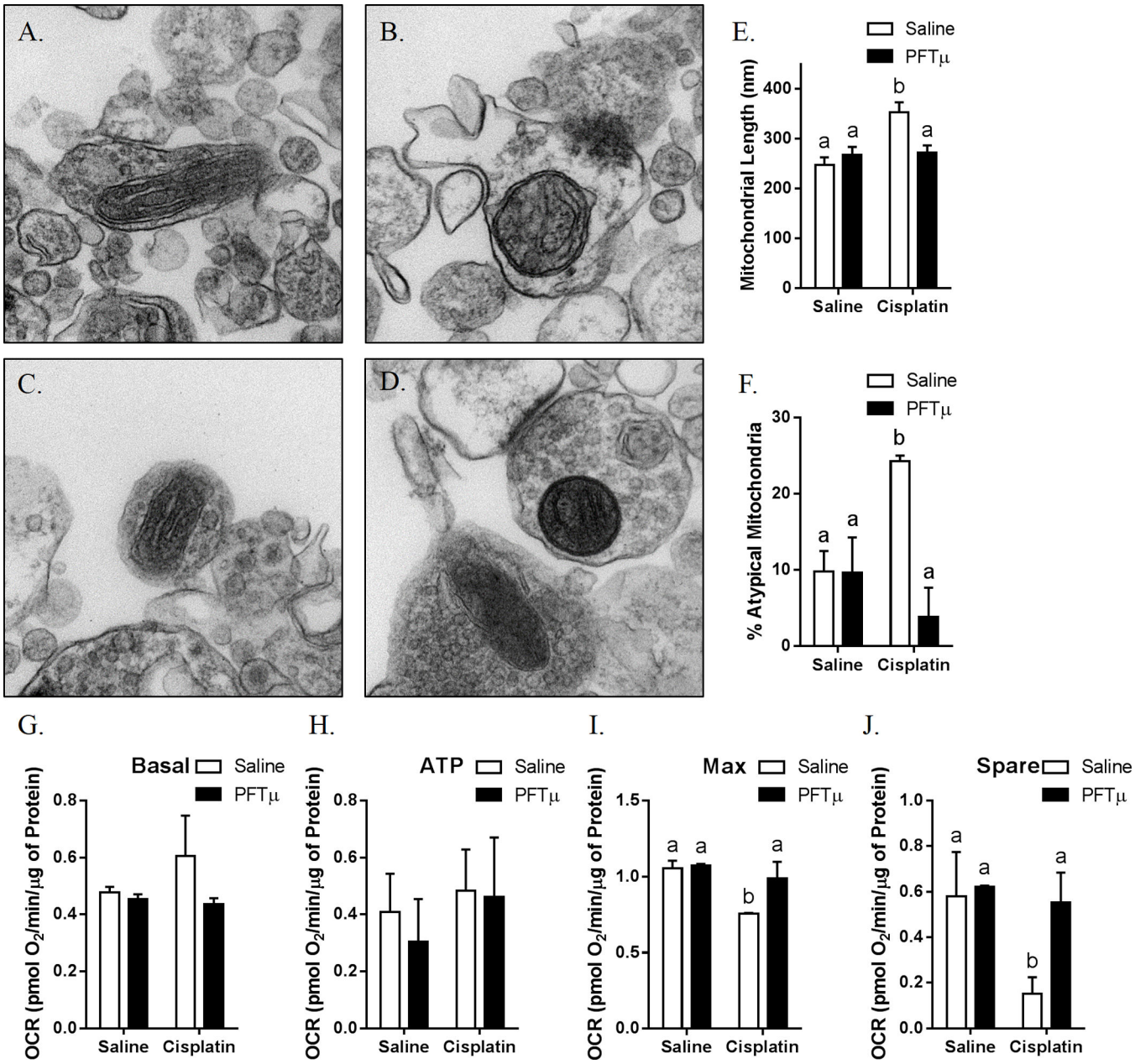

Figure 5. Effects of cisplatin and PFT-μ on mitochondrial morphology

*S*ynaptosomes were isolated from the brains of animals treated with **(A)** PBS, **(B)** cisplatin, **(C)** PFT-μ, or **(D)** PFT-μ plus cisplatin for two 5-day cycles. **(E)** Mitochondrial length and **(F)** percentage of atypical mitochondria were quantified. Results are expressed as means ± SEM; n = 8. Bars without a common superscript are significantly different ($P < 0.05$). Oxygen consumption rates were analyzed in isolated synaptosomes using the Seahorse XFe 24 Analyzer. **(G)** Basal, **(H)** ATP production-related, **(I)** maximum, and **(J)** spare respiratory capacity were calculated. Results are expressed as means ± SEM; n = 8. Bars without a common superscript are significantly different ($P < 0.05$).

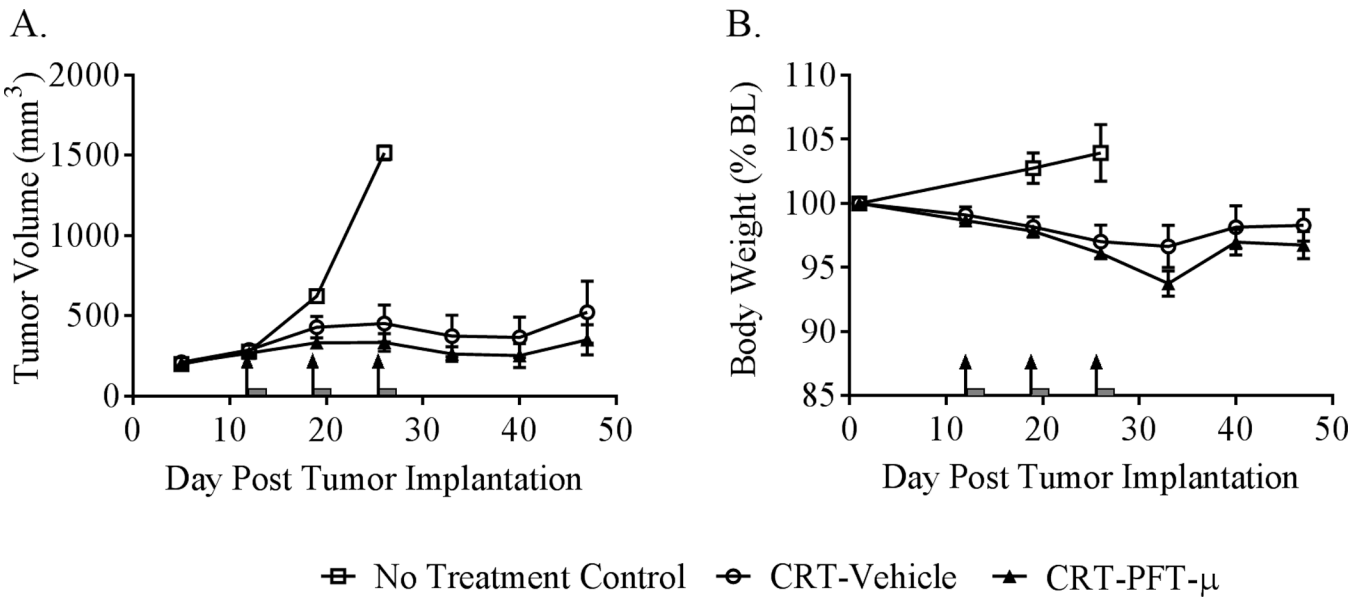

Figure 6. Effects of PFT-μ on the tumor's response to cancer therapy

Mice were implanted with a syngeneic murine model of HPV-positive head and neck cancer and were treated once weekly for 3 weeks with a regimen of cisplatin + local radiation (CRT). This regimen of CRT effectively delayed tumor growth, and this effect was not adversely affected by concurrent treatment with PFT-μ **(A)**. A repeated-measures ANOVA revealed a significant effect of time, $P < 0.01$, with no significant effect of group or group-by-time interaction. As anticipated, CRT resulted in mild weight loss that was not significantly exacerbated by PFT-μ treatment **(B)**. A repeated-measures ANOVA showed a significant effect of time, $P < 0.001$, with no significant effect of group or group-by-time interaction. Results are expressed as means ± SEM; n = 6. Arrows indicate day of CRT treatment; grey bars indicate PFT-μ treatment.

Table 1

Effect of cisplatin on the inflammatory response in the brain

Region	Gene	Saline	Cisplatin
24h post-treatment			
Hippocampus	IL-1β	1.00 (0.10)	0.75 (0.05)*
	IL-6	1.00 (0.12)	1.15 (0.11)
	TNFα	1.00 (0.13)	0.80 (0.08)
	GFAP	1.00 (0.06)	0.87 (0.03)*
	CD11b	1.00 (0.05)	0.86 (0.04)*
Prefrontal Cortex	IL-1β	1.00 (0.16)	0.97 (0.09)
	IL-6	1.00 (0.06)	0.91 (0.07)
	TNFα	1.00 (0.37)	0.73 (0.11)
	GFAP	1.00 (0.06)	0.81 (0.01)*
	CD11b	1.00 (0.05)	0.80 (0.17)
7d post-treatment			
Hippocampus	IL-1β	1.00 (0.22)	1.06 (0.25)
	IL-6	1.00 (0.30)	1.44 (0.28)
	TNFα	1.00 (0.07)	0.76 (0.05)*
	GFAP	1.00 (0.10)	1.03 (0.14)
	CD11b	1.00 (0.15)	1.03 (0.14)
Prefrontal Cortex	IL-1β	1.00 (0.08)	0.88 (0.13)
	IL-6	1.00 (0.13)	1.15 (0.06)
	TNFα	1.00 (0.18)	1.07 (0.30)
	GFAP	1.00 (0.03)	1.20 (0.24)
	CD11b	1.00 (0.04)	1.02 (0.10)